Green Chemistry

ARTICLE

The Synthesis of Di-carboxylate Esters Using Continuous Flow Vortex Fluidics

Received 00th January 20xx,
Accepted 00th January 20xx

DOI: 10.1039/x0xx00000x

www.rsc.org/

Joshua Britton,[a] Stuart B. Dalziel [b] and Colin L. Raston [a]

A vortex fluidic device (VFD) is effective in mediating the synthesis of di-esters at room temperature. Processing under ambient conditions allows for a simple and efficient synthesis, whilst operating under continuous flow addresses scalability. The rotational speed of the sample tube and the flow rate were critical variables during reaction optimization, and this relates to the behaviour of the fluid flow at a molecular level. Whilst at specific rotational speeds the tube imparts a vibrational response into the fluid flow, the flow rate dictates residence time and the ability to maintain high levels of shear stress. The combination of mechanically induced vibrations, rapid micromixing, high levels of shear stress and water evaporation results in yields up to 90% for 3.25 minutes or less residence time. These results are key for devising greener and more efficient processes both mediated by the VFD and other continuous flow platforms.

Introduction

Designing synthetic protocol to reduce the environmental impacts associated with organic chemistry is of paramount importance.[1, 2] Flow chemistry has impacted a number of syntheses,[3-5] improving both reaction yields and chemo/ regio-selectivity. Performing synthetic transformations in continuous flow can address both reaction scalability and efficiency. The benefits of using dynamic thin films in continuous flow processing include; (i) even and rapid heat dissipation, (ii) increased mass transfer, (iii) reaction homogeneity and (iv) limited reactor clogging.

Di-esters have a plethora of uses including: polymers,[6] agrochemicals, [7] skin cleaning agents,[8] and cellulosic based drugs.[9] Traditional *"round bottom flask"* approaches to synthesizing these chemicals include: microwave radiation with immobilized enzymes,[10] layered double hydroxides,[11] metallic nano-particles[12] and transition metals.[13, 14] Although these approaches are effective, they often require high reaction temperatures, prolonged reaction times and scalability is often not addressed. Recently, we reported that vibrations native to the VFD, improved chemical reactivity through generation of Faraday waves.[15] We envisaged that these vibrations might also facilitate a room temperature, continuous flow synthesis of di-carboxylate esters. We herein use a room temperature thin film flow chemistry approach to synthesize di-carboxylate esters in up to 90% yield for a residence time of 3.25 minutes or less.

The VFD is a continuous flow platform that processes reagents within thin films.[14] The thickness of the thin film (≈ 250 μm) depends upon the rotational speed, tilt angle, θ, diameter and height (length) of the sample tube. Computer controlled syringe pumps deliver reagents through metallic jet feeds into the hemisphere of the rotating sample tube that rotates up to 10,000 rpm. The height of the feed jets can be adjusted so that reagents can be released at different positions along the sample tube. This type of methodology was used to create a molecular assembly line approach to the synthesis of a local anaesthetic, lidocaine.[16]

Once the reagents are released from the jet feeds, the fluid impacts on the rotating glass tube. Whilst the liquid is not rotating at this point, it rapidly accelerates as it makes contact with the base of the rotating tube. The thin film is then thrown outwards by centrifugal force, much like a related spinning disk processor.[17] This fluid then feeds the Stewartson layers that form on the sidewall of the rotating sample tube. For a vertical

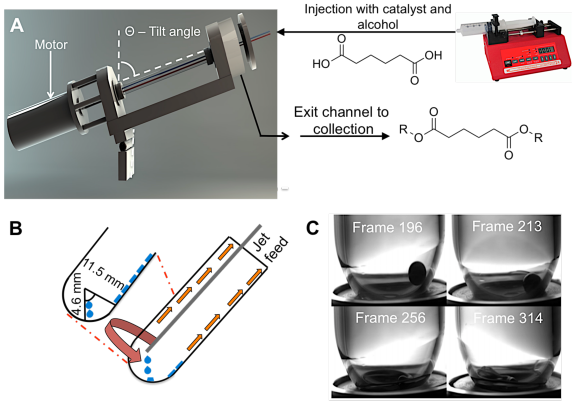

Fig. 1. (A) Schematic of the VFD showing the mode of entry of reagents into the rotating tube *via* a syringe pump. **(B)** Schematic of the drop regime in the 17.7 mm internal diameter VFD tube (as a 20 mm external diameter NMR tube). **(C)** High speed photographs (5400 fps, non consecutive frames) of a drop of water hitting the hemispherical part of such a tube, offset from the central axis, i.e. at a 45 degree tilt angle relative to the horizontal position. One revolution accounts for close to 68 frames. Full schematics and intricate workings of the VFD have been published previously.[16]

[a] *Centre for NanoScale Science and Technology, School of Chemical and Physical Sciences, Flinders University, Bedford Park, South Australia, 5045, E-mail: Colin.Raston@flinders.edu.au*
[b] *Department of Applied Mathematics and Theoretical Physics, University of Cambridge, UK, CB3 0WB*

† This research was supported by Flinders University, the University of Cambridge, the Government of South Australia and the Australian Research Council
Electronic Supplementary Information (ESI) available. See DOI: 10.1039/x0xx00000x

tube, θ = 90°, the film is expected to maintain an approximately paraboloidal shape; hence the name "vortex fluidic device". Inclining the tube on a tilt angle (Fig.1.) perturbs this equilibrium and imparts a gravitationally driven circulation.[18] During continuous flow, the liquid whirls up the rotating sample tube and exits in a controlled manner through a Teflon housing unit. The sample is then collected and quenched, or passed into another VFD for sequential processing.

The rotating sample tube is held firmly between two bearings. As all bearings contain imperfections, rotating the sample tube generates vibrations within the bearings that directly imparted on the sample tube. At specific rotational speeds, a harmonic vibration is generated that delivers a secondary fluid dynamic response in the form of a Faraday wave.[15] Faraday waves are created when a body of liquid is subjected to an oscillatory acceleration normal to its surface. Whilst microwaves [19] and ultrasonic vibrations [20-26] have been used in synthetic chemistry, there is no precedent for Faraday waves enhancing chemical reactions apart from those occurring within a VFD. The combination of Faraday waves and continuous flow chemistry is effective in the synthesis of di-carboxylate esters at room temperature.

Results and Discussion

Rotational speed considerations

First, the concentration of sulphuric acid needed to generate a response that could be further optimized was found. Given that there is limited catalyst recycling under plug flow conditions in the VFD under continuous flow, one equivalent of the acid was used. In previous work, we found that sulphuric acid was the superior catalyst for room temperature esterifications.[27] Even though there may be concerns with using this catalyst, it may be recycled.[28, 29] We believe that the short reaction times presented here, without applying thermal energy strikes a careful balance between reaction efficiency and sustainability. The rotational speed of the sample tube was then varied; there is a complex relationship between rotational speed and yield that originates from vibrational induced effects as previously mentioned. In order to explain these effects, it is important to understand how reagents are processed within the VFD.

As a droplet of reagent exits the jet feed and strikes the bottom of the rotating sample tube the fluid forms a boundary layer whereby the fluid experiences rapid micromixing and high levels of shear stress. The droplet then radiates from the impact spot and enters the thin film. Once entered, the reagents experience the effect of Faraday waves that are present at very specific rotational speeds. The events described above likely increase the reaction rate through rapid mixing, hence allowing much shorter reaction times. The higher yields obtained in this work is likely to be a result of removal of the water by-product. We hypothesized that the large surface area of the thin film could increase the rate of evaporization of water, enhancing the position of equilibrium towards the ester. In testing this, 2.0 mL of water was processed in the confined mode of operation of the VFD, and the water loss monitored. Over a 20-minute time period, VFD-mediated water loss occurred at around 500 μmoles second^{-1}, whilst under non-VFD-mediated conditions this rate dropped to 100 μmoles second^{-1} (Fig. S1). This finding is consistent with the esterification of fats and oils using the VFD whereby quantitative yields are obtained in sub-minute residence times at room temperature.[27] Rapid micromixing plays a more substantial role in biodiesel generation, due to the biphasic nature of the system.[27]

In the present study, various rotational speeds result in higher yields. This is hypothesized to arise from the presence of Faraday waves and the properties they impart on the fluid flow. Only at very specific rotational speeds are enhancements observed (eg. 6950 rpm) compared to a non-VFD-mediated solution (Fig 3). In the non-VFD-mediated solution, the exact same solution was left to react for one hour in a round bottom flask, resulting in a 69% yield. This yield is presumably limited by the equilibrium conditions reached. We stipulate that when processing in the absence of Faraday waves, high shear stress levels only exist in the boundary layer (at the bottom of the sample tube). At specific rotational speeds, Faraday waves are generated in the thin films that increase micromixing with shorter diffusion paths throughout the system. These effects create a system with greater reactivity, and through water loss out of the thin film, the position of equilibrium is enhanced, resulting in the overall VFD-mediated enhancement.

The magnitude of the enhancement will depend on the nature of the flow at the molecular scale. For weak macroscopic shear, we expect molecular collisions to be dominated by Brownian motion, but for strong shear, the shear rate will dominate. The fluid entering the Ekman-layer will experience high shear stress, and while this is intense, a given fluid parcel is only exposed to it briefly before it radiates away from the impact point. The fluid then drains into the thin film perturbing the walls of the sample tube. However, at specific rotational speeds, Faraday waves can exist in the fluid flow. For Faraday waves of frequency ω, wave length, λ and amplitude a, the shear rate

$$(1)\ |S| \sim \frac{a}{\lambda}\omega,$$

may be smaller than that in the boundary layer, but the period of time in which the fluid is exposed to it is magnitudes of order longer, and of course, this is directly controlled by the flow rate of reagents through the VFD. Accordingly, when a Faraday wave is present there is likely to be shorter diffusion paths and increased micro mixing, with a concomitant increase in the rate of reaction.

Variation in the contact angle of sample tube also affects the reaction outcome. This presumably arises from the perturbation of the fluid flow at the molecular level. The inner surface of the sample tubes was covalently coated with a dodecylsilane treatment. This created a hydrophobic surface that had a noticeable effect on the VFD-mediated response (Fig. 3B and D). Similar for both the coated and non-coated sample tubes, the rotational speeds tested from 4000 to 5500 rpm gave a decrease in VFD-mediated yields. This arises from alcohol

evaporation from the thin film (*vide infra)*, removing a primary reactant, noting that this is consistent with the high surface area of thin films present in the VFD.

Reagent delivery into a hydrophilic sample tube[15] (Fig. 3A and C) established the optimal rotational speed of 6950 rpm for enhancement of the reaction. This is slightly different to reagent delivery into a hydrophobic tube, with a shift in optimal rotational speed to 7000 rpm (Fig. 3B and D). Given that these rotational speeds are similar, but not exact, the surface coating has a direct effect on the optimal rotational speed. The rotational landscape is less erratic when reagent delivery occurs on the wall of the sample tube (Fig. 3C and D). This suggests that some phenomenon exists in the hemisphere of the sample tube that contributes further to VFD-mediated enhancement.

The majority of VFD-mediated reactions use standard borosilicate sample tubes with reagents delivery occurring in the hemisphere at the base of the tube. At the rotational speeds of 6000, 6400, 6650 and 6950 rpm there is VFD-mediated enhancement. This presumably arises from a harmonic vibration creating a Faraday wave within the sample tube. The Faraday wave which results, is hypothesised to prolong high shear stress on the reagents, increase micromixing and shorten reaction paths, all contributing to the observed increase in yield.

An emerging concept in VFD flow chemistry is the ability to alter the fluids surface tension during processing. At the microscale, high shear stress rates lead to changes in the fluids surface tension. The changing surface tension could facilitate the removal of water, thus enhancing the position of equilibrium (*vide supra*). Indeed, we observe a condensate forming on the jet feeds and exit tubing during VFD processing. The room temperature removal of the water by-product may explain the VFD-based equilibrium enhancement compared to a non-VFD-mediated solution. This is a phenomenon that we are currently exploring in detail.

Flow rate considerations

Understanding the effect of flow rate allows the design of more efficient continuous flow protocol. Typically, the flow rate determines the residence time of reagents; however, through this work we have discovered that flow rate plays an important role in micromixing and the level of shear stress generated. In synthesizing di-esters, the flow rate, Q, was varied from 0.20 mL/min to 1.00 mL/min and the yield monitored (Fig.4) A range of di-acids (C_5-C_{10}) and alcohols (methanol, ethanol, *n*-propanol and *n*-butanol) were chosen as reaction partners. The results indicate that the flow rate is highly important for reaction optimization. In maturing an understanding of this phenomenon, we now develop a model of the fluid flow in the VFD.

The feed stream containing the reactants is introduced at a mean flow rate, Q, through a metal feed tube of radius r_n (internal diameter - 2.04 mm). Although Q is continuous, surface tension promotes the formation of droplets at the tip of the needle. A droplet grows in size until its weight is sufficient to overcome the capillary forces to break the fluid film. This occurs when the droplet radius reaches

$$(2)\ a = \left(\frac{3\gamma r_n}{2\rho g}\right)^{\frac{1}{3}}$$

where ρ is the density of the fluid, γ is the surface tension of the fluid and g is the acceleration due to gravity. For $Q = 0.50$ mL/min, this equation predicts around 30 drops per minute. This prediction matched the experimental outcome for methanol. Each drop falls vertically from the tip of the needle and lands in the hemisphere end of the rotating sample tube (Fig. 2). A viscous Stokes boundary layer of scale thickness

$$(3)\ \delta = \left(\frac{\nu}{\Omega}\right)^{\frac{1}{2}},$$

forms at the base of the droplet, with the fluid in it accelerating azimuthally to experience a centrifugal force throwing it radially outward. Here, ν is the kinematic viscosity and Ω is the angular velocity of the tube. This expulsion of fluid (now rotating) from beneath the drop brings new fluid (not yet rotating) is in contact with the boundary in a manner similar to that found in an Ekman layer.[18] The fluid expelled from beneath the droplet drains radially in a spiralling motion with viscous stresses balancing the centrifugal force. The maximum shear stress experienced during the initial acceleration, scaled as

$$(4)\ \sigma = \rho(\nu\Omega^3)^{\frac{1}{2}},$$

although high shear is sustained as the fluid drains radially outwards and up the hemispherical end of the tube. The draining film eventually merges with the film of fluid coating the inside of the inclined rotating tube. The time taken for the fluid to drain out of the hemisphere plays a key role in setting the maximum flow rate. Through understanding how to maximize the shear stress on the reagents as they enter the

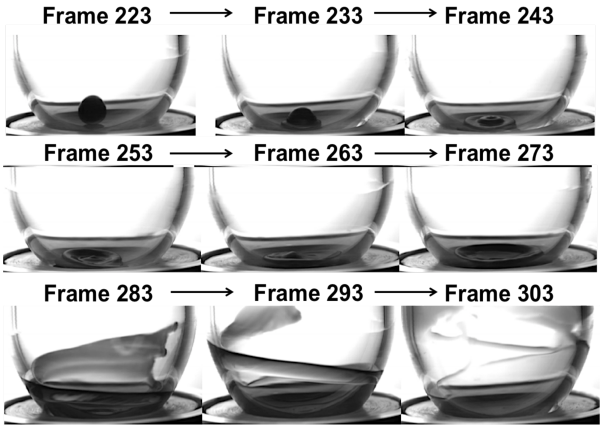

Fig. 2. High-speed images of a droplet of water colliding with the hemisphere of a 17.7 mm internal diameter dry borosilicate glass VFD sample tube. The tube is orientated at 90° relative to the horizontal position and rotating at 5250 rpm. Frame 253-263 - the thickening of the drop edge forming after initial impact. Frame 273 - the instability of the drop edge, leading to viscous fingering instability, frame 283-303. To generate these photographs a droplet of water mixed with blue dye was dropped from a height of 2.0 cm into the hemisphere of a sample tube at a 90° tilt angle. A high-speed camera was operating at 5400 fps, shown are non-consecutive frames.

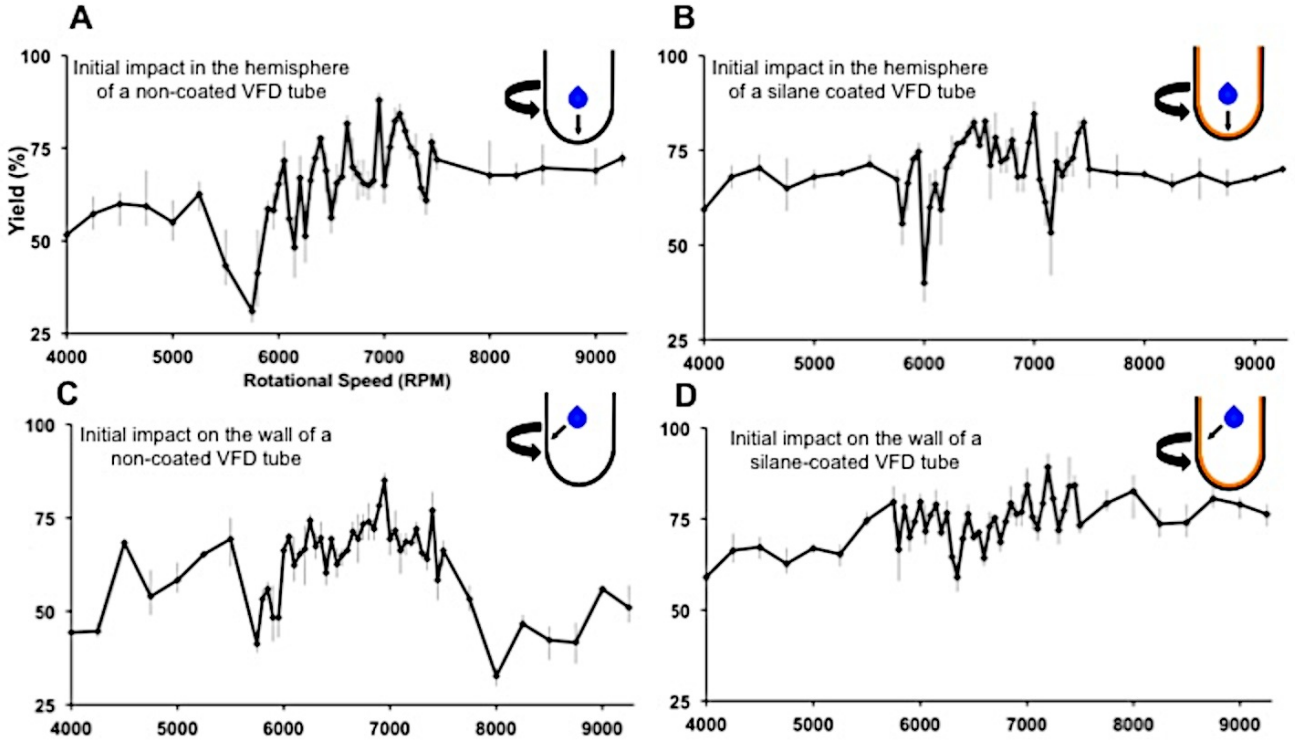

Fig. 3. The effect of sample tube rotational speed on the yield of di-methyladipate. The nature of the sample tube surface as well as the reagent entry regime were explored. A 0.45 mL/min flow rate was used at a tilt angle of 45°. **(A)** Mixing in the hemisphere of a hydrophilic, pristine boro-silicate glass NMR tube. **(B)** Mixing in the hemisphere of a hydrophobic, dodecyl silane-treated NMR tube. **(C)** Mixing on the wall of a hydrophilic, pristine boro-silicate glass NMR tube. **(D)** Mixing on the wall of a hydrophilic, dodecylsilane treated glass NMR tube. The average yield is reported here with the maximum and the minimum of the data set indicated as error (n=3). Larger 250-rpm increments were sampled from 4000 rpm to 5750 rpm as all previous chemical transformation have occurred within the 6000-8000 rpm range, and this is a focus in the present study. Treatment of borosilicate glass to create a hydrophobic surface has been previously reported.[15] All experimental results shown above were carried out on more than two different VFD's to make sure this was not a device specific enhancement, and thus the error indicated takes into account small, device specific effects.

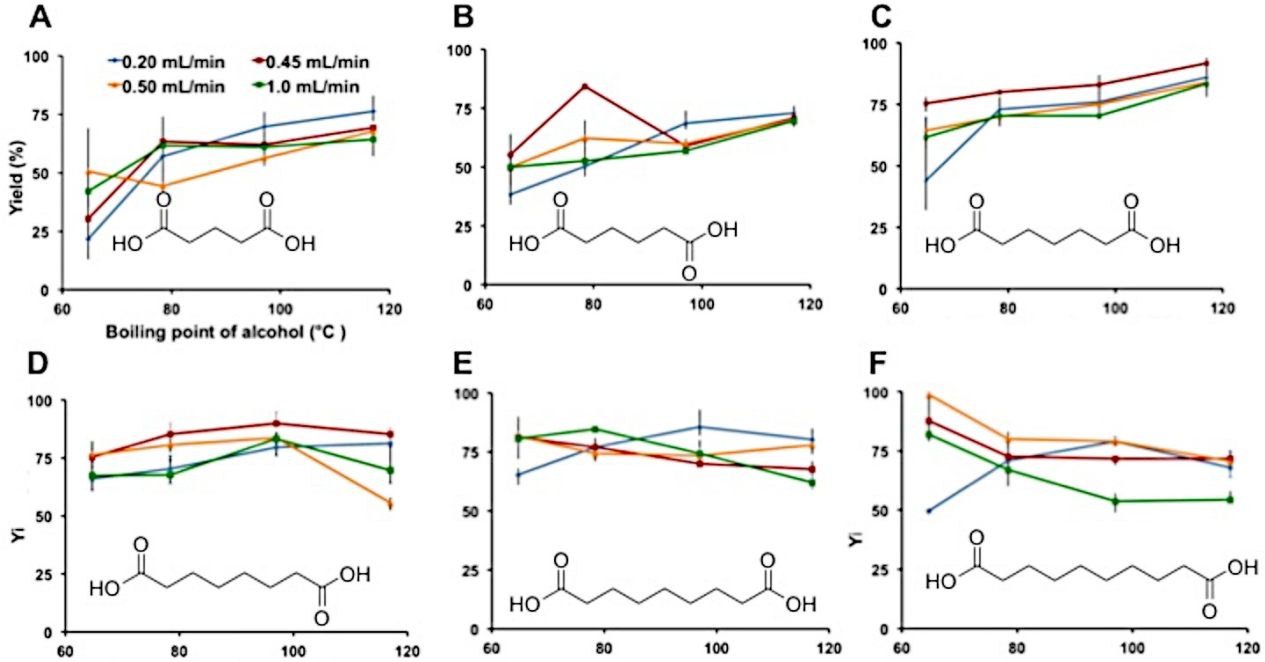

Fig. 4. The yields obtained the for esterification of various of di-acids with various alcohols (x-axis); **(A)** Glutaric acid, **(B)** Adipic acid, **(C)** Pimelic acid, **(D)** Suberic acid, **(E)** Azelaic acid, and **(F)** Sebasic acid undergoing esterification. The VFD was operated at a rotational speed of 5250 rpm and at a 45-degree tilt angle, θ. Each data point is an average and the error bars shown are the error of the maximum and minimum of the data set (n=3). A rotational speed of 5250 rpm was used so that other phenomenon had little effect on the observations. This allows a comparison to be made without other VFD-based effects interplaying. Boiling points of the solvents used: methanol - 64.7°C, ethanol – 78.4°C, n-propanol- 97°C and n-butanol- 117.4°C. All experiments shown above were carried out on more than two different VFD's to make sure this was not a device specific enhancement, and thus the error indicated takes into account small, device specific effects.

VFD, more efficient reaction design can be achieved, helping to generate more efficient processing. The droplet itself is accelerated into the established thin film on a time scale

$$(5)\ \tau = a/(\nu\Omega)^{\frac{1}{2}},$$

whereas the thickness of the remnant film decreases gradually as

$$(6)\ h \sim (\frac{\nu}{\Omega^2 t})^{\frac{1}{2}},$$

which emphasizes that it could take a long time for the thin film to flow (drain) from the hemisphere and into the thin film up the tube, leading to different shearing rates within the rotating tube. Based purely on the acceleration phase, these scaling arguments predict a reactant feed upper limit of

$$(7)\ \mathrm{Q} \sim a^2(\nu\Omega)^{\frac{1}{2}}$$

that is around an order of magnitude greater than the optimal conditions found here. This suggests that as expected, many parameters affect the optimal flow rate. Exceeding this limit will change the principle balance and lead to an accumulation of fluid in the base of the tube which leads to an inefficient continuous flow process and possibly the formation of by-products in chemical processes in general. Such an effect is detrimental to the green chemistry metrics associated with a reaction.

The drainage of the fluid influences the environment in which the next droplet experiences as it impacts the rotating tube. If the incoming droplet spreads on a dry surface, then capillary forces can dominate the behaviour of the drop. Capillary forces can give rise to a viscous fingering instability, decreasing the time that shear force can interplay with the reactants. This potential for instability does not require the surface to be dry *per se*, but nevertheless this directly influences the critical radius at which the instability occurs. When this instability forms, the fluid drains into rivulets that carry the fluid outward more rapidly, decreasing the time that the fluid parcel is subjected to high shear stress. On the assumption that the high shear stresses are beneficial, this situation is undesirable for the performance of the VFD. Ensuring that the surface of the VFD is wet, and that it does not dry out between successive droplets, will help increase the time that the reagents are exposed to high shear stress levels, and theoretically this should increase reactivity.

When viscous fingering instability does not occur, a remnant fluid film from the previous drop reduces the shear stress experienced by the new drop entering the system. If the surface does not dry out between droplets, we can approximate this as a continuous flow process onto the surface. The resulting film also experiences some instability. Ignoring surface tension, it is known that instabilities occur on a flat rotating disk when the flow rate exceeds [18]

$$(8)\ \mathrm{Q}_c = \frac{5\pi g\nu}{3\Omega^2},$$

but numerically this is some two orders of magnitude less than the regime in which we are operating. In the VFD, however, the hemispherical end to the tube means that a component of the centrifugal force (scaling as $\Omega^2 r$ at radius r) plays a similar role to gravity on the flat disk, but dominates over gravity as r increases. Using this idea suggests the stability boundary scales as

$$(9)\ \mathrm{Q}_c \sim r\nu.$$

Our optimal flow rates slightly exceed this if we take $r = a$, the radius of the droplet, but is slightly below it when r is taken to be the radius of the tube. This suggests our optimal conditions are very close to the stability boundary, if continuous flow is assumed. In the present context, it is noteworthy that the scale for the initial film thickness ranges from 35 to 76 μm, while maximum shear stress estimates increase with viscosity from 14 Pa for methanol to 31 Pa for *n*-butanol. These values are independent of *Q*. This is observed in our experimental findings (Fig. 4A-B), whereby the flow rate has little effect on the yield of the esters. Generally, for the shorter chain di-acids, higher boiling solvents give higher yields. This presumably arises from the increase in shear stress with viscosity. The optimal flow rate changes as longer, more hydrophobic acids are esterified. Esterification of short carbon chain di-acids (C_5-C_6, Fig. 4A-B) has no optimal flow rate, for reasons discussed above. However, for longer chain di-acids (C_7-C_8) this trend diminishes and the yield becomes more a function of the flow rate, with a 0.45 mL/min flow rate providing the highest yields for all alcohols tested.

In designing further reactions, and taking into account the information presented above, the maximum flow rate must also be considered. If the flow rate exceeds a certain threshold, the underlying fluid dynamics changes due to instabilities within the film will become evident. Residence time in the VFD tube follows a decay inverse relationship, with higher flow rates resulting in only a slight decrease in residence time. This has been previously determined through experimental, not theoretical means, but matched predicted models.[27]

$$\text{Residence time} = 152.37\ \mathrm{Q}^{-0.934}$$

where Q is the flow rate (ml/min) of reagents through the rotating tube.

Conclusion

We have developed an understanding of how important the rotational speed and flow rate is in VFD-mediated continuous flow synthesis. In conventional flow chemistry, the flow rate is often not finely optimized as it primarily controls residence time. However, in VFD-mediated processes, finely controlling the flow rate can maintain high levels of shear stress, leading to more efficient synthesis. The rotational speed of the tube dictates when a harmonic vibration is reached, and thus when a

Table 1. A comparison of VFD-mediated and current methods for esterifying di-acids. Examples from the literature allow a direct comparison to the VFD-mediated process that has a generally shorter reaction time for comparable yields. 'Batch' is for a non-VFD mediated processing. The 'reaction time' for the VFD is the time taken for a finite volume of liquid delivered to the base of the tube to exit the top. *Yield not specified in manuscript.

Di-acid: alcohol	Batch or VFD	Catalyst	Temperature (°C)	Reaction time (mins)	Yield (%)
C_6: Methanol	VFD	Acid	RT	3.25	89
C_6: Methanol [30]	Batch	Polymer	RT	720	95
C_6: Methanol [31]	Batch	Lipase	58.5	358	100
C_7: n-Butanol	VFD	Acid	RT	3.25	92
C_7: Ethanol	VFD	Acid	RT	3.25	85
C_8: Ethanol[32]	Batch	Acid	Microwave	3.00	70
C_9: Ethanol	VFD	Acid	RT	3.25	78
C_9: Ethanol [33]	Batch	Acid	231	480	*
C_9: n-Butanol	VFD	Acid	RT	3.25	78
C_9: n-Butanol[34]	Batch	SiO_2/Al_2O_3	117	180	95

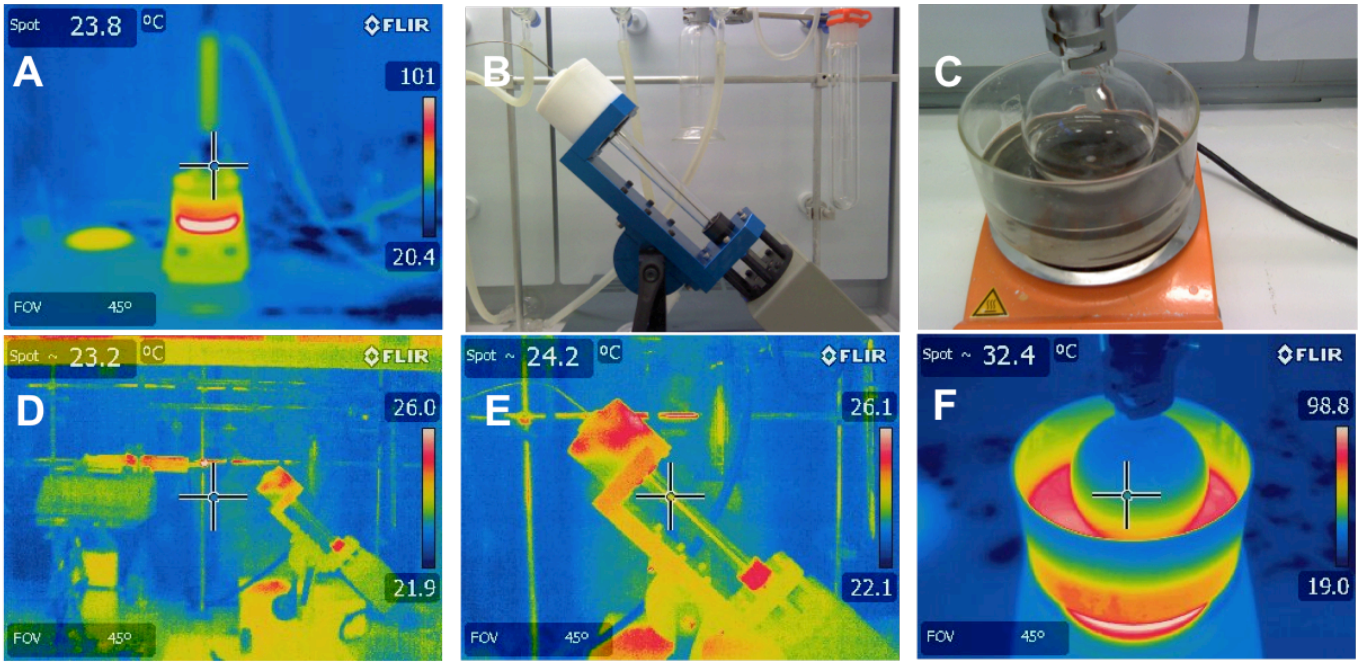

Parameter	Batch	VFD
Electricity consumption	825 W	100 W
Water consumption	300 mL min^{-1}	-

Fig. 4. Comparative thermal images for a traditional batch type esterification *vs*. a VFD-mediated esterification. For the batch type reaction, a 100 mL of n-propanol in a 250 mL round bottom flask was used to demonstrate thermal variance. A silicone oil bath was used set at 100 °C. Water usage was calculated using a traditional condensing unit. The slowest flow of water was used to keep the condenser at a low temperature. This was a slow flow rate, but 300 mL min^{-1} was consumed. (**A**) Showing the thermal IR image for reflux in a round bottom flask, (**B**) photograph of the VFD during use, (**C**) photograph of a traditional round bottom flask set up, (**D**) A thermal image of the VFD set up after 25 minutes of operation, (**E**) a thermal image of photograph **B**, and (**F**) a thermal image of photograph **C**. This figure allows a visual comparison to demonstrate how energy efficient the VFD is compared to traditional processes. The thermal IR camera was a FLIR thermal imagining camera, Lens - 10 mm IR thermal. The hot plates used to calculate energy consumption are Radleys carousel hotplate (240 V, 50 Hz, 825 W min^{-1}.) The VFD runs using 0.4 A at a 6950 rpm rotational speed. The syringe pump uses a 12 V power supply with a 0.75 A.

Faraday wave is induced into the thin film. By optimizing the rotational speed and flow rate, yields that are comparable to those from previous work are obtained, but now with remarkably shorter reaction times and greater simplicity of the processing, while addressing the vexing question of scalability (Table 1). Overall, this work is destined to impact on flow chemistry in highlighting the importance of flow rates in chemical processes, and in general the importance of fine-tuning reaction conditions under flow.

Experimental Section

A di-acid (6.83 mmol, 1 eq.), alcohol (30 mL) and sulphuric acid (6.83 mmol, 1 eq.) were loaded into a syringe pump. The choice of the volume of alcohol was governed by sebasic acid (C_{10}) dissolving only in a minimum of 30 mL of *n*-butanol, and thus when using 30 mL of alcohol all di-acids were the same concentration. The 17.7 mm internal diameter sample tube (borosilicate glass, as a standard NMR tube) was inclined at a tilt angle of 45° relative to the horizontal position. The solution was then injected into the rotating tube *via* a stainless steel jet feed using a computer controlled syringe pump at the required flow rate. The feed jet was situated 11.5 mm away from the lower wall of the inclined tube and 4.6 mm from the bottom of the hemispherical base of the tube. The tube was rotated about its axis at various speeds, and the solution collected on an ice bath with excess alcohol then removed under reduced pressure immediately post VFD processing. The residue was taken up in diethyl ether and further washed with water (1 x 25 mL), 2 M NaOH (1 x 25 mL) and then dried with $MgSO_4$. The resulting di-ester solution was filtered and taken to dryness under reduced pressure.

Diethyl ether was used in these experiments so that the solution could be purified without loss of the volatile ester. More sustainable solvents can be used in isolation processes, but fear of loosing the ester product led us to use an easily removable solvent with a boiling point far below the generated esters. As noted by a referee, diethyl ether should be avoided at all costs, both in industrial and academic environments. Magnesium sulphate was also used to remove water from the solution so that this would not affect the calculated yields. If other isolation procedures were used then magnesium sulphate and sodium hydroxide solutions could be avoided. However, as this was a more fundamental research exercise, this method was favoured over distillation and other classical work up procedures.

Spectroscopy. ^{1}H and ^{13}C NMR were obtained on a 600 MHz Bruker spectrometer. Typical quantitative conditions were used (Delayed pulse (D1)-10.00 and Number of scans -64) to ascertain the purity of the ester.

Acknowledgements

We acknowledge support from the Government of South Australia and the Australian Research Council.

1. J. Glaser, *Clean Technol. Envir.*, **2009**, 11, 371-374.
2. R. A. Sheldon, *Chem. Soc. Rev.*, **2012**, 41, 1437-1451.
3. S. J. Haswell and P. Watts, *Green Chem.*, **2003**, 5, 240-249.
4. C. Wiles and P. Watts, *Green Chem.*, **2012**, 14, 38-54.
5. J.-i. Yoshida, H. Kim and A. Nagaki, *ChemSusChem*, **2011**, 4, 331-340.
6. T. Yutaka, A. Tadanao, S. Tomoo and T. Kiyoshi, in *Agricultural and Synthetic Polymers*, American Chemical Society, 1990, vol. 433, ch. 12, pp. 136-148.
7. J. D. S. A. B. Kneževic-Stevanović, S. P. Šerbanovicć, I. R. Radovic and M. LJ. Kijevčanin, *J. Serb. Chem. Soc.*, **2014**, 79, 77-87.
8. *USA Pat.,* US5891449 A, 1999.
9. N. Kar, H. Liu and K. J. Edgar, *Biomacromolecules*, **2011**, 12, 1106-1115.
10. M. Risso, M. Mazzini, S. Kröger, P. Saenz-Méndez, G. Seoane and D. Gamenara, *Green Chemistry Letters and Reviews*, **2012**, 5, 539-543.
11. M. B. Abdul Rahman, U. H. Zaidan, M. Basri, M. Z. Hussein, R. N. Z. R. A. Rahman and A. B. Salleh, *J. Mol. Catal. B-Enzym*, **2008**, 50, 33-39.
12. P. S. Rathore, J. Advani, S. Rathore and S. Thakore, *J. Mol. Catal. A-Chem*, **2013**, 377, 129-136.
13. H. Urata, D. Goto and T. Fuchikami, *Tetrahedron Lett.*, **1991**, 32, 3091-3094.
14. R. Thakkar and U. Chudasama, *Green Chemistry Letters and Reviews*, **2009**, 2, 61-69.
15. J. Britton, S. B. Dalziel and C. L. Raston, *RSC Adv.*, **2015**, 5, 1655-1660.
16. J. Britton, J. M. Chalker and C. L. Raston, *Chem-Eur. J.*, **2015**, 21, 10660-10665.
17. X. Chen, N. M. Smith, K. S. Iyer and C. L. Raston, *Chem. Soc. Rev.*, **2014**, 43, 1387-1399.
18. H. P. Greenspan, *The Theory Of Rotating Fluids*, Cambridge University Press, Cambridge, 1968.
19. P. Lidström, J. Tierney, B. Wathey and J. Westman, *Tetrahedron*, **2001**, 57, 9225-9283.
20. G. Cravotto and P. Cintas, *Chem-Eur J.*, **2007**, 13, 1902-1909.
21. D. Yu, L. Tian, H. Wu, S. Wang, Y. Wang, D. Ma and X. Fang, *Process Biochem*, **2010**, 45, 519-525.
22. K. S. Suslick, *Sci. Am.*, **1989**, 260, 80-86.
23. A. K. Singh, S. D. Fernando and R. Hernandez, *Energ. Fuels*, **2007**, 21, 1161-1164.
24. C. Leonelli and T. J. Mason, *Chem. Eng. Process: Process Intensification*, **2010**, 49, 885-900.
25. C. Pétrier, A. L. Gemal and J.-L. Luche, *Tetrahedron Lett.*, **1982**, 23, 3361-3364.
26. R. B. N. Baig and R. S. Varma, *Chem. Soc. Rev.*, **2012**, 41, 1559-1584.
27. J. Britton and C. L. Raston, *RSC Adv.*, **2015**, 5, 2276-2280.
28. W. L. Klotz, Google Patents, 1998.
29. G. Stucki, K. W. Hanselmann and R. A. Hürzeler, *Biotechnology and Bioengineering*, **1993**, 41, 303-315.
30. S. Bhunia, B. Banerjee and A. Bhaumik, *Chem. Comm.*, **2015**, 51, 5020-5023.
31. N. Chaibakhsh, M. B. Abdul Rahman, M. Basri, A. B. Salleh and R. N. Z. R. A. Rahman, *Biocatal.Biotransfor.*, **2009**, 27, 303-308.
32. WO 2012011123, 2012.
33. S.-J. Zhang and W.-X. Hu, *Med. Chem. Res.*, **2012**, 21, 3312-3320.
34. N. G. Grigor'eva, A. M. Suleimanova, M. R. Agliullin and B. I. Kutepov, *Russ. J. Appl Chem+*, **2014**, 87, 773-779.